THE JOURNAL OF PHYSICAL CHEMISTRY Letters

Letter

Cite This: J. Phys. Chem. Lett. 2018, 9, 1312−1317

pubs.acs.org/JPCL

Specific Substates of Ras To Interact with GAPs and Effectors: Revealed by Theoretical Simulations and FTIR Experiments

Yang Li,[†,⊥] Yuwei Zhang,[†] Frederik Großerüschkamp,[§] Sara Stephan,[§] Qiang Cui,[‡] Carsten Kötting,[§] Fei Xia,*[,†,∥] and Klaus Gerwert*[,§]

[†]School of Chemistry and Molecular Engineering, East China Normal University, Shanghai 200062, China

[‡]Department of Chemistry and Theoretical Chemistry Institute, University of Wisconsin, 1101 University Avenue, Madison, Wisconsin 53706, United States

[§]Department of Biophysics, Ruhr-University Bochum, ND 04 North, 44780 Bochum, Germany

[∥]NYU-ECNU Center for Computational Chemistry at NYU Shanghai, Shanghai 200062, China

[⊥]School of Information Science and Engineering, Shandong Agricultural University, Taian 271018, China

Supporting Information

ABSTRACT: The oncogenic Ras protein adopts various specific conformational states to execute its function in signal transduction. The large number of Ras structures obtained from X-ray and NMR experiments illustrates the diverse conformations that Ras adopts. It is difficult, however, to connect specific structural features with Ras functions. We report the free-energy landscape of Ras·GTP based on extensive explicit solvent simulations. The free-energy map clearly shows that the functional state 2 of Ras·GTP in fact has two distinct substates, denoted here as "$Tyr32_{in}$" and "$Tyr32_{out}$". Unbiased MD simulations show that the two substrates interconvert on the submicrosecond scale in solution, pointing to a novel mechanism for Ras·GTP to selectively interact with GAPs and effectors. This proposal is further supported by time-resolved FTIR experiments, which demonstrate that Tyr32 destabilizes the Ras·GAP complex and facilitates an efficient termination of Ras signaling.

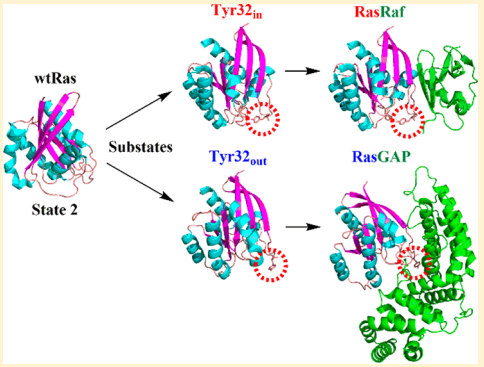

The Ras protein participates in a series of important signal transduction processes in cells, and its malfunction often leads to tumors.[1,2] It is well known that Ras is a molecular switch that can adopt an "on" or an "off" state to regulate its interaction with upstream or downstream kinases.[3] The active Ras can interact with effectors such as Raf to conduct the signal downstream. On the contrary, switching of Ras from the active to inactive state is controlled by the GTP hydrolysis to GDP in Ras; the hydrolysis activity can be accelerated by several orders of magnitude by interacting with GTPase activating proteins (GAPs).[4] To understand the functions of Ras and interactions with other kinases, many researchers have made an effort to obtain the 3D structure of Ras by means of various experimental techniques such as X-ray crystallography and NMR.[5−18] Until now, more than 100 structures of isolated Ras with GTP, GDP, and analogues such as GppNHp as well as its mutants have been obtained, and their structures have been deposited in the Protein Data Bank online (Section 1, SI). However, the functional implication of divergent conformations[19] of Ras is still not fully understood. In this work, we report a comprehensive simulation study of conformational states adopted by Ras·GTP in solution. The results lead to the proposal that the "on" state of Ras·GTP consists of two interconverting substates that preferentially interact with GAPs and effectors, respectively. This dynamic scenario for the regulation of Ras function is further verified by time-resolved Fourier-transform infrared spectroscopy (FTIR).[20−27]

In 1990, Pai et al.[5] reported the crystal structure of Ras in complex with the GTP analogue GppNHp, where the hydroxyl oxygen atom of residue Thr35 coordinates to the Mg^{2+} ion at the active site of Ras and the hydroxyl group of Tyr32 points outward. Later, it was first revealed by Geyer et al. using ^{31}P NMR spectroscopy that the complex Ras·GppNHp exists in two main conformational states, termed state 1 and state 2.[10] A series of following NMR studies by Kalbitzer and co-workers[11−15] and FTIR studies[27] demonstrated that Ras in complex with GTP and its analogues indeed exists in two conformational states in equilibrium; the wildtype Ras·GTP complex was predominantly in state 2 at the experimental temperature 278 K.[15] Kalbitzer et al.[14] proposed that state 1 of Ras represents the conformation interacting with guanine nucleotide exchange factor (GEF) and that Ras has a minimal number of eight functional states to complete the GTP cycle.[28] The existence of state 1 of Ras has been supported by the crystal structure (PDB ID: 4EFL) of Muraoka et al.;[29] the structure is characterized by the broken hydrogen-bond

Received: February 1, 2018
Accepted: February 28, 2018
Published: February 28, 2018

DOI: 10.1021/acs.jpclett.8b00342
J. Phys. Chem. Lett. 2018, 9, 1312−1317

interactions between Thr35 and Mg^{2+} ion as well as between Tyr32 and oxygen atom in the γ-group of triphosphate of GTP. The loop in the switch I region in state 1 also exhibits large thermal fluctuation, as indicated by the B-factors. As for state 2, the crystal structures available for wildtype Ras such as 5P21,[5] 1CTQ,[7] 1QRA,[7] 1P2S,[16] 3RRY,[17] 4DLR,[18] 3L8Y,[30] and 3L8Z[30] show the distinct conformational divergence in the switch I region, especially for the orientations of residue Tyr32.

Numerous molecular simulations were carried out to characterize the structural features of conformations[31−33] of Ras·GTP as well as Ras·GDP, the conformational transition[34,35] between Ras·GTP ND Ras·GDP, and the dynamic evolution of Ras mutants.[36−40] However, it remains unclear which specific conformation Ras·GTP adopts in solution to preferentially interact with GAP or effectors when it is in state 2.[15] To reveal the specific conformational features of Ras·GTP in state 2, we performed extensive replica-exchange molecular dynamics (REMD)[41] simulation (Section 2, SI) to explore the conformational distribution of Ras·GTP in solution using the simulation package Gromacs 4.5.5.[42,43] Distinguished from these previous efforts,[31−40] our work aims to establish an explicit connection between specific conformations and functional states of Ras.

We used the crystal structure of Ras in state 2 (PDB ID: 3L8Z) as the initial structure and Amber99sb force field[44] as the potential function; the substrate GppNHp was substituted by GTP to construct the Ras·GTP complex. The whole system was then immersed in a cubic water box with 6902 water molecules and the solution environment was set to be physiological with 0.155 mol/L of NaCl. A total number of 84 replicas was used in the REMD simulation, with the sampling temperatures ranging from 278 to 430 K. The simulation time for each replica at each temperature is 200 ns and the cumulative trajectory length is 16.8 μs. On the basis of the trajectories sampled at 278 K, we projected the free-energy landscape onto the 2D space (Figure 1) spanned by root-mean-square deviation (RMSD) and the radius of gyration (R_g).

Figure 1 shows that the two free-energy basins are well-separated, approximately located in regions with the RMSD values of 0.1 to 0.33 and 0.33 to 0.40 nm, respectively. Because the reference structure (3L8Z) is believed to represent state 2,

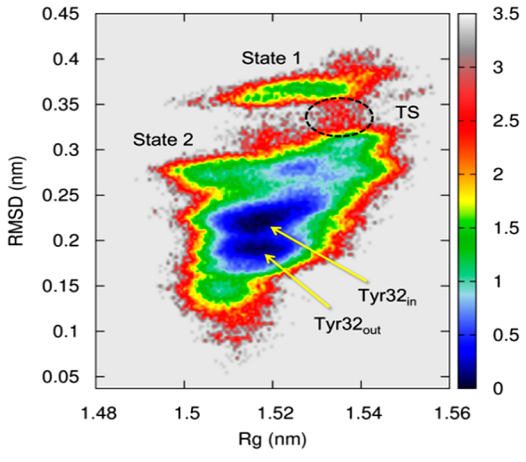

Figure 1. Constructed 2D free-energy contour of Ras at 278 K with respect to RMSD relative to 3L8Z and R_g of all atoms in Ras. The transition-state (TS) region connects state 1 and state 2. State 2 features two substates, denoted by $Tyr32_{in}$ and $Tyr32_{out}$, respectively. The units of RMSD and R_g are in nanometers and free energy ΔG is in kcal/mol.

it is sensible to postulate that the basin located at the larger RMSD of 0.33 to 0.40 nm represents state 1.[29] To verify this, we extracted the structures from this basin and conducted clustering analysis on these structures (Section 3, SI). It was found that the major representative structure obtained by clustering analysis is indeed similar to the crystal structure 4EFL, with its loop regions exhibiting large fluctuations. The free-energy difference $\Delta\Delta G_{12}$ between states 2 and 1 from the free-energy surface is approximately −1.40 kcal/mol, which is in agreement with the value of −1.33 kcal/mol measured from the NMR experiment.[15] The TS connecting the two basins is located at the region with the RMSD of 0.33 nm and R_g of 1.54 nm. Because the free-energy barrier is likely notably higher than k_BT, sampling of the TS region in the free-energy map is not as extensive as that for the free-energy basins.

A notable feature of the free-energy surface in Figure 1 is that state 2 is featured with two adjacent subbasins with similar energetics. To characterize the structures representing the two substates, we performed clustering analysis on the structures extracted from these subbasins and least-squares fitting with crystal structures of state 2. The analysis indicates that the major structure to represent the top subbasin is similar to the structure 3L8Z (Section 4, SI), with the hydroxyl group of Tyr32 pointing to GTP; thus the substate is denoted as "$Tyr32_{in}$". Meanwhile, the major structure to represent the bottom subbasin resembles the crystal structure 1QRA (Section 5, SI), with Tyr32 pointing into solution; thus the substate is denoted as "$Tyr32_{out}$". In other words, we postulate that the structures 3L8Z and 1QRA represent two distinct substates of isolated Ras. Both structures were also found in previous MD simulations.[45] To support the hypothesis further, we collected a set of crystal structures for isolated wildtype Ras and performed a least-squares fit with each other. The overlapped structures in Figure 2a) show that the Tyr32 residues in these structures prefer either "in" or "out" orientations, in accord with the observation of two subbasins for state 2 in Figure 1. Notably, all of these structures are featured with the stable coordination of Thr35 to Mg^{2+} ion, no matter whether Tyr32 stays "in" or "out". Thus the stable coordination of Thr35 to Mg^{2+} could be considered as one of the fingerprints for state 2; this is supported by the observation that the mutation T35A led to the shift of equilibrium toward state 1.[15]

To explore the time scale associated with the dynamic conversion between $Tyr32_{in}$ and $Tyr32_{out}$ substates, we performed an unbiased 2 μs all-atom MD simulation for isolated Ras in solution at the experimental temperature 278 K.[15] The crystal structure of 3L8Z[30] was chosen as the initial conformation in solution. More details of the MD simulation are provided in Section 2 of the SI. Figure 2b shows the measured distance between the oxygen atom of γ-phosphate in GTP and hydrogen atom of hydroxyl of Tyr32 during the simulation. The hydroxyl group of Tyr32 forms stable hydrogen-bonding interaction with one oxygen atom of the γ-phosphate of GTP during the first 320 ns, and Ras stays in the $Tyr32_{in}$ substate. After that, the hydrogen bond is broken and Tyr32 moves away from GTP, as indicated by the increased distance between them. Subsequently, Ras stays in the $Tyr32_{out}$ substate for 500 ns and then transforms back to the $Tyr32_{in}$ substate spontaneously at 820 ns. The snapshots extracted from the MD trajectory in Figure 2c illustrate the conversion between the two substates. The closest distance between the hydroxyl oxygen of Tyr32 and the GTP γ-oxygen atom from the MD snapshots is 0.27 nm, the same as the value of 0.27 nm

DOI: 10.1021/acs.jpclett.8b00342
J. Phys. Chem. Lett. 2018, 9, 1312−1317

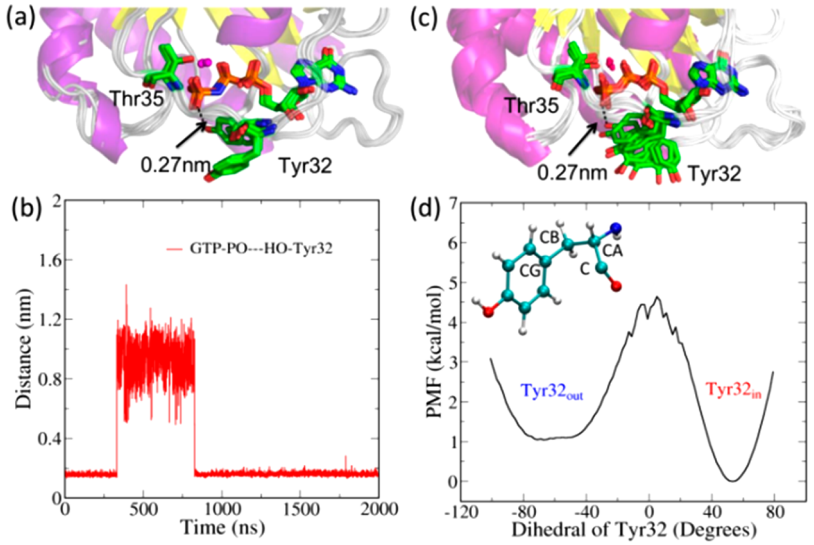

Figure 2. (a) Cartoon representation of overlapped structures of isolated Ras, with the PDB IDs: 5P21, 1CTQ, 1QRA, 1P2S, 3L8Y, 3L8Z, 3RRY, and 4DLR. The heavy atoms in 3L8Z were taken as the reference for least-squares fitting. (b) Measured distances between the O atom of γ-group in GTP and H atom of the hydroxyl group of Tyr32 during a 2 μs MD trajectory. (c) Schematic representation of switching of Tyr32 between "in" and "out" using the snapshots taken from the MD trajectory. (d) Calculated potential of mean force (PMF) for the interconversion of $Tyr32_{out}$ and $Tyr32_{in}$ substates by projecting the REMD trajectory on the reaction coordinate of the dihedral C-CA-CB-CG of Tyr32 residue.

observed in the crystal structure of 3L8Y.[30] Furthermore, the calculated potential mean force with respect to the dihedral of Tyr32 in Figure 2d shows that the conversion of $Tyr32_{in}$ to $Tyr32_{out}$ needs to overcome a barrier of 4.5 kcal/mol to break the H-bonding interaction of the P−O group of GTP and H−O group of Tyr32. The substate $Tyr32_{out}$ appears to be less stable than $Tyr32_{in}$ by 1 kcal/mol.

The comparison of extensive MD simulations with Ras crystal structures strongly indicates that the isolated Ras in solution adopts two substates in state 2 with subtle structural differences. What functions are associated with these two substates? In previous NMR studies by Spoerner et al.,[15] the state of Ras complexed with effectors has been assigned as state 2 because it exhibits the spectroscopic character similar to the free Ras in solution. Later, the state of Ras complexed with GAP was assigned as state 3 with the high-pressure NMR.[28] The $Tyr32_{in}$ and $Tyr32_{out}$ characterized by our analyzed structures from simulation might correspond to the state 2 and state 3 found in the NMR experiments. We hypothesize that Ras adopts the $Tyr32_{in}$ substate to interact with effectors such as Raf for downstream signal transduction and adopts the $Tyr32_{out}$ substate to interact with GAPs for GTP hydrolysis. This proposal is postulated on the basis of comparison of known crystal structures of isolated Ras with the Ras complexes. It is found that the crystal structure of isolated Ras in 1QRA is similar to that of Ras in the RasGAP complex of 1WQ1[6] with a RMSD of 0.0505 nm (Section 6, SI); moreover, $Tyr32_{out}$ is considered as the specific substate to interact with GAP because Tyr32 needs to move out to let the arginine finger of GAP rotate into the cleft for GTP hydrolysis. On the contrary, the structure of Ras in 3L8Z is similar to that in RasRaf of 4G0N,[46] with an RMSD of 0.0531 nm (Section 6, SI), which shows that Tyr32 points inward as the β2 sheet of Ras interacts with Raf.

To test our hypothesis regarding the role of Tyr32 in determining the functions of the two substates of Ras, we performed FTIR experiments (Section 7, SI) with the Ras Y32A mutant and compared them with Ras wildtype. The time course of the GAP-catalyzed hydrolysis reaction is considerably affected by the mutation of Tyr32. For wildtype three rates were observed.[26] Instead of these three rates we can resolve only two rates in the GAP-catalyzed reaction of Ras Y32A. The comparisons of the amplitude spectra clearly show that the first rate corresponds to the processes observed during the first two rates of wildtype. After these rates in both cases the protein-bound Pi is formed.[25] This can be seen in Figure 3, where the time course of the marker band for this state at 1186 cm^{-1} is shown. The slowest rate k_3 corresponds to the Pi release, and the absorption of the Pi intermediate vanishes.

The comparison of the rate constants shows that the protein-bound intermediate is formed faster by a factor of 2 when the Tyr32 is absent. This is in agreement with the presence of a $Tyr32_{in}$ population, where the Tyr needs to be pushed out for the GAP interaction. Another explanation would be that Tyr32 is destabilizing the Ras·GAP complex. Interestingly an even stronger kinetic effect is found for the Pi-release. Here the mutant is slower by a factor of 5. Thus Tyr32 induces a faster cleavage of the Ras·GAP complex. In turn the GAP protein is available for switching off another Ras much earlier, leading to a more efficient termination of Ras signaling.

The experimental data obtained by FTIR support our hypothesis. In brief, a schematic illustration of how Ras function depends on its conformational features is shown in Figure 4. The cartoon representations of RasGAP, RasRaf, and RasGEF complexes are drawn using the crystal structures with the PDB IDs 1WQ1,[6] 4G0N,[46] and 1BKD.[47] The wildtype Ras possesses two specific $Tyr32_{out}$ and $Tyr32_{in}$ substates in state 2, in which Ras can interact with GAPs for GTP hydrolysis and effectors for signal transduction. The two substates can interconvert to each other on the submicrosecond time scale as residue Tyr32 moves into or out of the catalytic cleft of Ras. Meanwhile, Ras also can adopt state 1 to interact with GEF for the exchange of GTP and GDP. The equilibrium between state 2 and state 1 occurs on a time scale of seconds, as observed in NMR experiments.[15]

DOI: 10.1021/acs.jpclett.8b00342
J. Phys. Chem. Lett. 2018, 9, 1312−1317

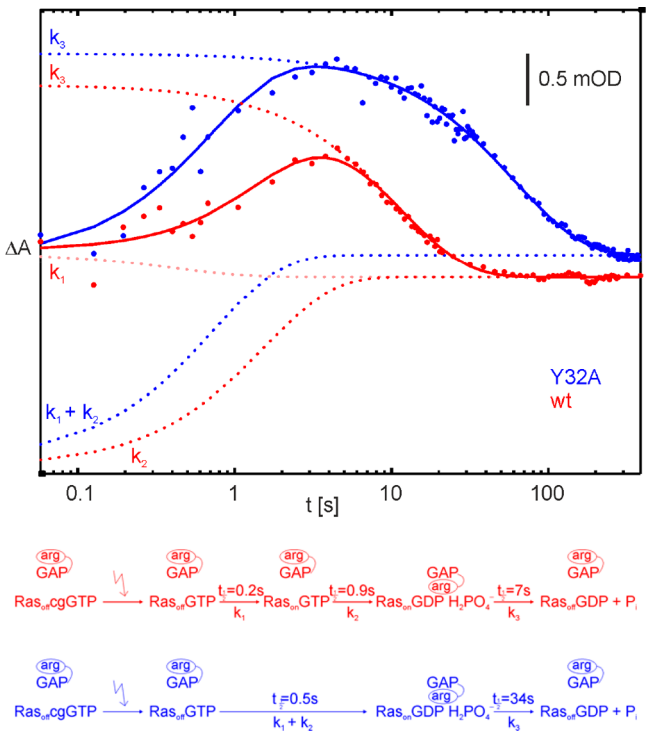

Figure 3. Time-dependent absorbance changes of a marker band for the protein-bound $H_2PO_4^-$ intermediate during the GAP-catalyzed hydrolysis reaction of Ras wt (red) and Ras Y32A (blue). As indicated in the scheme in the lower part of the Figure, this intermediate is much more stable without Tyr32, indicating that this residue interferes with Ras GAP binding.

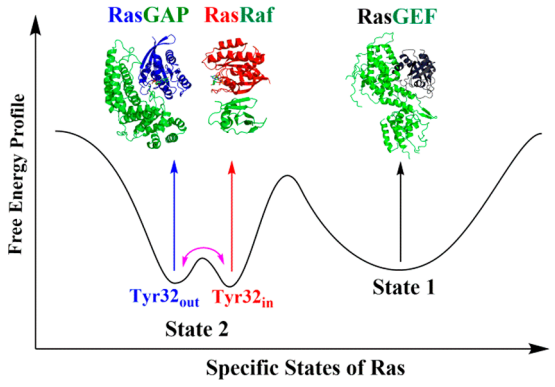

Figure 4. Schematic illustration of specific conformational states of Ras associated with its functions, where the purple double-headed arrow indicates the interconversion between the $Tyr32_{out}$ and $Tyr32_{in}$ substates.

Finally, the significant conclusions drawn from this work are summarized below. First, the 2D free-energy surface provides detailed energetics associated with the conformational distribution of isolated Ras as well as a solid basis for understanding the structural divergence of Ras obtained by various experimental techniques so far, especially for differentiating state 1 and state 2. Second, the constructed free-energy surface reveals two subbasins for state 2, which correspond to the $Tyr32_{in}$ and $Tyr32_{out}$ substates that are supported by the existing crystal structures. The two substates differ from each other mainly in the orientation of Tyr32, and their interconversion was observed to occur on a submicrosecond time scale in unbiased MD simulations. Third, analysis of the simulation results in the context of available crystal structures leads to the hypothesis that Ras adopts the $Tyr32_{in}$ substate to interact with effectors and the $Tyr32_{out}$ substate to interact with GAPs. The hypothesis was supported by the results of FTIR spectroscopy. Therefore, the current study reveals a dynamic mechanism through which Ras regulates its interaction with other proteins to fulfill its functions. The results also provide new clues to the design of Ras inhibitors[30] and mechanistic study of GTP hydrolysis[48−54] in Ras.

■ ASSOCIATED CONTENT

Supporting Information

The Supporting Information is available free of charge on the ACS Publications website at DOI: 10.1021/acs.jpclett.8b00342.

PDB IDs of isolated Ras and mutants, details of REMD and MD simulations, results of clustering analyses, and comparison of crystal structures of Ras and its complexes. (PDF)

■ AUTHOR INFORMATION

Corresponding Authors

*F.X.: E-mail: fxia@chem.ecnu.edu.cn.

*K.G.: E-mail: gerwert@bph.rub.de.

ORCID

Qiang Cui: 0000-0001-6214-5211

Carsten Kötting: 0000-0002-3599-9657

Fei Xia: 0000-0001-9458-9175

Author Contributions

Y.L., Y.Z., Q.C., and F.X. performed theoretical simulations. F.G., S.S., C.K., and K.G. performed FTIR experiments.

Notes

The authors declare no competing financial interest.

■ ACKNOWLEDGMENTS

This work was supported by the National Natural Science Foundation of China (grant nos. 21773065, 21433004, and 11747006), Natural Science Foundation of Shandong (ZR2016BB13), and Deutsche Forschungsgemeinschaft SFB 642 TP A1. Q.C. acknowledges partial support from the National Institutes of Health grant 7R01GM106443. We acknowledge the support of the NYU-ECNU Center for Computational Chemistry at NYU Shanghai. We also thank the supercomputer center of ECNU for providing computer time.

■ REFERENCES

(1) Cox, A. D.; Der, C. J. Ras History: the Saga Continues. *Small GTPases* **2010**, *1*, 2−27.

(2) Wittinghofer, A.; Waldmann, H. Ras − A Molecular Switch Involved in Tumor Formation. *Angew. Chem., Int. Ed.* **2000**, *39*, 4192−4214.

(3) Vetter, I. R.; Wittinghofer, A. The Guanine Nucleotide-Binding Switch in Three Dimensions. *Science* **2001**, *294*, 1299−1304.

(4) Wittinghofer, A.; Vetter, I. R. Structure-function Relationships of the G domain, a Canonical Switch Motif. *Annu. Rev. Biochem.* **2011**, *80*, 943−971.

(5) Pai, E. F.; Krengel, U.; Petsko, G. A.; Goody, R. S.; Kabsch, W.; Wittinghofer, A. Refined Crystal Structure of the Triphosphate Conformation of H-Ras p21 at 1.35Å Resolution: Implications for the Mechanism of GTP Hydrolysis. *EMBO J.* **1990**, *9*, 2351−2359.

(6) Scheffzek, K.; Ahmadian, M. R.; Kabsch, W.; Wiesmuller, L.; Lautwein, A.; Schmitz, F.; Wittinghofer, A. The Ras-RasGAP Complex: Structural Basis for GTPase Activation and its Loss in Oncogenic Ras Mutants. *Science* **1997**, *277*, 333−338.

DOI: 10.1021/acs.jpclett.8b00342
J. Phys. Chem. Lett. 2018, 9, 1312−1317

(7) Scheidig, A. J.; Burmester, C.; Goody, R. S. The Pre-Hydrolysis State of p21(ras) in Complex with GTP: New Insights into the Role of Water Molecules in the GTP Hydrolysis Reaction of Ras-like Proteins. *Structure* **1999**, *7*, 1311−1324.
(8) Schweins, T.; Geyer, M.; Scheffzek, K.; Warshel, A.; Kalbitzer, H. R.; Wittinghofer, A. Substrate-assisted Catalysis as a Mechanism for GTP Hydrolysis of p21ras and Other GTP-binding Proteins. *Nat. Struct. Biol.* **1995**, *2*, 36−44.
(9) Wang, J. H.; Xiao, D. G.; Deng, H.; Callender, R.; Webb, M. R. Vibrational Study of Phosphate Modes in GDP and GTP and their Interaction with Magnesium in Aqueous Solution. *Biospectroscopy* **1998**, *4*, 219−227.
(10) Geyer, M.; Schweins, T.; Herrmann, C.; Prisner, T.; Wittinghofer, A.; Kalbitzer, H. R. Conformational Transitions in p21ras and its Complexes with the Effector Protein rafRBD and the GTPase Activating Protein GAP. *Biochemistry* **1996**, *35*, 10308−10320.
(11) Spoerner, M.; Wittinghofer, A.; Kalbitzer, H. R. Perturbation of the Conformational Equilibria in Ras by Selective Mutations as Studied by ^{31}P NMR Spectroscopy. *FEBS Lett.* **2004**, *578*, 305−310.
(12) Spoerner, M.; Nuehs, A.; Ganser, P.; Herrmann, C.; Wittinghofer, A.; Kalbitzer, H. R. Conformational States of Ras Complexed with the GTP Analogue GppNHp or GppCH$_2$p: Implications for the Interaction with Effector Proteins. *Biochemistry* **2005**, *44*, 2225−2236.
(13) Spoerner, M.; Nuehs, A.; Herrmann, C.; Steiner, G.; Kalbitzer, H. R. Slow Conformational Dynamics of the Guanine Nucleotide-Binding Protein Ras Complexed with the GTP Analogue GTPγS. *FEBS J.* **2007**, *274*, 1419−1433.
(14) Kalbitzer, H. R.; Spoerner, M.; Ganser, P.; Hozsa, C.; Kremer, W. Fundamental Link between Folding States and Functinal States of Proteins. *J. Am. Chem. Soc.* **2009**, *131*, 16714−16719.
(15) Spoerner, M.; Hozsa, C.; Poetzl, J.; Reiss, K.; Ganser, P.; Geyer, M.; Kalbitzer, H. R. Conformational States of Human Rat sarcoma (Ras) Protein Complexed with its Natural Ligand GTP and their Role for Effector Interaction and GTP Hydrolysis. *J. Biol. Chem.* **2010**, *285*, 39768−39778.
(16) Buhrman, G.; de Serrano, V.; Mattos, C. Organic Solvents Order the Dynamics Switch II in Ras Crystals. *Structure* **2003**, *11*, 747−751.
(17) Buhrman, G.; O'Connor, C.; Zerbe, B.; Kearney, B. M.; Napoleon, R.; Kovrigina, E. A.; Vajda, S.; Kozakov, D.; Kovrigin, E. L.; Mattos, C. Analysis of Binding Site Hot Spots on the Surface of Ras GTPase. *J. Mol. Biol.* **2011**, *413*, 773−789.
(18) Holzapfel, G.; Buhrman, G.; Mattos, C. Shift in the Equilibrium between On and Off States of the Allosteric Switch in Ras-GppNHp Affected by Small Molecules and Bulk Solvent Composition. *Biochemistry* **2012**, *51*, 6114−6126.
(19) Lu, S.; Jang, H.; Muratcioglu, S.; Gursoy, A.; Keskin, O.; Nussinov, R.; Zhang, J. Ras Conformational Ensembles, Allostery, and Signaling. *Chem. Rev.* **2016**, *116*, 6607−6665.
(20) Cepus, V.; Scheidig, A. J.; Goody, R. S.; Gerwert, K. Time-Resolved FTIR Studies of the GTPase Reaction of H-Ras p21 Reveal a Key Role for the β-phosphate. *Biochemistry* **1998**, *37*, 10263−10271.
(21) Allin, C.; Gerwert, K. Ras Catalyzes GTP Hydrolysis by Shifting Negative Charges from γ- to β-phosphate as Revealed by Time-Resolved FTIR Difference Spectroscopy. *Biochemistry* **2001**, *40*, 3037−3046.
(22) Allin, C.; Ahmadian, M. R.; Wittinghofer, A.; Gerwert, K. Monitoring the GAP Catalyzed H-Ras GTPase Reaction at Atomic Resolution in Real Time. *Proc. Natl. Acad. Sci. U. S. A.* **2001**, *98*, 7754−7759.
(23) Kötting, C.; Gerwert, K. Time-Resolved FTIR Studies Provide Activation Free Energy, Activation Enthalpy and Activation Entropy for GTPase Reactions. *Chem. Phys.* **2004**, *307*, 227−232.
(24) Kötting, C.; Gerwert, K. Proteins in Action Monitored by Time-Resolved FTIR Spectroscopy. *ChemPhysChem* **2005**, *6*, 881−888.
(25) Kötting, C.; Blessenohl, M.; Suveyzdis, Y.; Goody, R. S.; Wittinghofer, A.; Gerwert, K. A Phosphoryl Transfer Intermediate in the GTPase Reaction of Ras in Complex with its GTPase-Activating Protein. *Proc. Natl. Acad. Sci. U. S. A.* **2006**, *103*, 13911−13916.
(26) Kötting, C.; Kallenbach, A.; Suveyzdis, Y.; Wittinghofer, A.; Gerwert, K. The GAP Arginine Finger Movement into the Catalytic Site of Ras Increases the Activation Entropy. *Proc. Natl. Acad. Sci. U. S. A.* **2008**, *105*, 6260−6265.
(27) Kötting, C.; Kallenbach, A.; Suveyzdis, Y.; Eichholz, C.; Gerwert, K. Surface Change of Ras Enabling Effector Binding Monitored in Real Time at Atomic Resolution. *ChemBioChem* **2007**, *8*, 781−787.
(28) Kalbitzer, H. R.; Rosnizeck, I. C.; Munte, C. E.; Narayanan, S. P.; Kropf, V.; Spoerner, M. Intrinsic Allosteric Inhibition of Signaling Proteins by Targeting Rare Interaction States Detected by High Pressure NMR Spectroscopy. *Angew. Chem., Int. Ed.* **2013**, *52*, 14242−14246.
(29) Muraoka, S.; Shima, F.; Araki, M.; Inoue, T.; Yoshimoto, A.; Ijiri, Y.; Seki, N.; Tamura, A.; Kumasaka, T.; Yamamoto, M.; Kataoka, T. Crystal Structure of the State 1 Conformations of the GTP-bound H-Ras Protein and its Oncogenic G12V and Q61L Mutants. *FEBS Lett.* **2012**, *586*, 1715−1718.
(30) Rosnizeck, I. C.; Spoerner, M.; Harsch, T.; Kreitner, S.; Filchtinski, D.; Herrmann, C.; Engel, D.; König, B.; Kalbitzer, H. R. Metal-Bis(2-picolyl)amine Complexes as State 1(T) Inhibitors of Activated Ras Protein. *Angew. Chem., Int. Ed.* **2012**, *51*, 10647−10651.
(31) Gorfe, A. A.; Grant, B. J.; McCammon, J. A. Mapping the Nucleotide and Isoform-Dependent Structural and Dynamical Features of Ras Proteins. *Structure* **2008**, *16*, 885−896.
(32) Kobayashi, C.; Saito, S. Relation between the Conformational Heterogeneity and Reaction Cycle of Ras: Molecular Simulation of Ras. *Biophys. J.* **2010**, *99*, 3726−3734.
(33) Kapoor, A.; Travesset, A. Differential Dynamics of RAS Isoforms in GDP- and GTP-bound States. *Proteins: Struct., Funct., Genet.* **2015**, *83*, 1091−1106.
(34) Ma, J.; Karplus, M. Molecular Switch in Signal Transduction: Reaction Paths of the Conformational Changes in Ras p21. *Proc. Natl. Acad. Sci. U. S. A.* **1997**, *94*, 11905−11910.
(35) Grant, B. J.; Gorfe, A. A.; McCammon, J. A. Ras Conformational Switching: Simulating Nucleotide-Dependent Conformational Transitions with Accelerated Molecular Dynamics. *PLoS Comput. Biol.* **2009**, *5*, e1000325.
(36) Lukman, S.; Grant, B. J.; Gorfe, A. A.; Grant, G. H.; McCammon, J. A. The Distinct Conformational Dynamics of K-Ras and H-Ras A59G. *PLoS Comput. Biol.* **2010**, *6*, e1000922.
(37) Futatsugi, N.; Tsuda, M. Molecular Dynamics Simulations of Gly-12→Val Mutant of p21^{ras}: Dynamic Inhibition Mechanism. *Biophys. J.* **2001**, *81*, 3483−3488.
(38) Sharma, N.; Sonavane, U.; Joshi, R. Differentiating the Pre-hydrolysis States of Wild-type and A59G Mutant Hras: An Insight through MD Simulations. *Comput. Biol. Chem.* **2017**, *69*, 96−109.
(39) Lu, S.; Jang, H.; Nussinov, R.; Zhang, J. The Structural Basis of Oncogenic Mutations G12, G13 and Q61 in Small GTPase K-Ras4B. *Sci. Rep.* **2016**, *6*, 21949.
(40) Sayyed-Ahmad, A.; Prakash, P.; Gorfe, A. A. Distinct Dynamics and Interaction Patterns in H- and K-Ras Oncogenic P-loop Mutants. *Proteins: Struct., Funct., Genet.* **2017**, *85*, 1618−1632.
(41) Sugita, Y.; Okamoto, Y. Replica-Exchange Molecular Dynamics Method for Protein Folding. *Chem. Phys. Lett.* **1999**, *314*, 141−151.
(42) Van der Spoel, D.; Lindahl, E.; Hess, B.; Groenhof, G.; Mark, A. E.; Berendsen, H. J. C. GROMACS: Fast, Flexible and Free. *J. Comput. Chem.* **2005**, *26*, 1701−1718.
(43) Hess, B.; Kutzner, C.; van der Spoel, D.; Lindahl, E. GROMACS 4: Algorithms for Highly Efficient, Load-Balanced, and Scalable Molecular Simulation. *J. Chem. Theory Comput.* **2008**, *4*, 435−447.
(44) Hornak, V.; Abel, R.; Okur, A.; Strockbine, B.; Roitberg, A.; Simmerling, C. Comparison of Multiple Amber Force Fields and Development of Improved Protein Backbone Parameters. *Proteins: Struct., Funct., Genet.* **2006**, *65*, 712−725.
(45) Rudack, T.; Xia, F.; Schlitter, J.; Kötting, C.; Gerwert, K. The Role of Magnesium for Geometry and Charge in GTP Hydrolysis,

DOI: 10.1021/acs.jpclett.8b00342
J. Phys. Chem. Lett. 2018, 9, 1312−1317

Revealed by Quantum Mechanics/Molecular Mechanics Simulations. *Biophys. J.* **2012**, *103*, 293−302.
(46) Fetics, S. K.; Guterres, H.; Kearney, B. M.; Buhrman, G.; Ma, B.; Nussinov, R.; Mattos, C. Allosteric Modulation of Ras-GTP is Linked to Signal Transduction through RAF Kinase. *Structure* **2015**, *23*, 505−516.
(47) Boriack-Sjodin, P. A.; Margarit, S. M.; Bar-Sagi, D.; Kuriyan, J. The Structural Basis of the Activation of Ras by Sos. *Nature* **1998**, *394*, 337−343.
(48) Schweins, T.; Geyer, M.; Kalbitzer, H. R.; Wittinghofer, A.; Warshel, A. Linear Free Energy Relationships in the Intrinsic and GTPase Activating Protein-Stimulated Guanosine 5′-Triphosphate Hydrolysis of p21ras. *Biochemistry* **1996**, *35*, 14225−14231.
(49) Glennon, T. M.; Villà, J.; Warshel, A. How Does GAP Catalyze the GTPase Reaction of Ras? A Computer Simulation Study. *Biochemistry* **2000**, *39*, 9641−9651.
(50) Klähn, M.; Rosta, E.; Warshel, A. On the Mechanism of Hydrolysis of Phosphate Monoesters Dianions in Solutions and Proteins. *J. Am. Chem. Soc.* **2006**, *128*, 15310−15323.
(51) Xia, F.; Rudack, T.; Cui, Q.; Kötting, C.; Gerwert, K. Detailed Structure of the $H_2PO_4^-$-Guanosine Diphosphate Intermediate in Ras-GAP Decoded from FTIR Experiments by Biomolecular Simulations. *J. Am. Chem. Soc.* **2012**, *134*, 20041−20044.
(52) Wallin, G.; Kamerlin, S. C. L.; Åqvist, J. Energetics of Activation of GTP Hydrolysis on the Ribosome. *Nat. Commun.* **2013**, *4*, 1733.
(53) Prasad, B. R.; Plotnikov, N. V.; Lameira, J.; Warshel, A. Quantitative Exploration of the Molecular Origin of the Activation of GTPase. *Proc. Natl. Acad. Sci. U. S. A.* **2013**, *110*, 20509−20514.
(54) Åqvist, J.; Kamerlin, S. C. L. Conserved Motifs in Different Classes of GTPases Dictate their Specific Modes of Catalysis. *ACS Catal.* **2016**, *6*, 1737−1743.

DOI: 10.1021/acs.jpclett.8b00342
J. Phys. Chem. Lett. 2018, 9, 1312−1317